

[Article ID] 1003- 6326(2002) 05- 0826- 03

# Properties of Zr-Ti-V-Mn-Ni hydride alloy<sup>①</sup>

WEN Ming-fen(文明芬)<sup>1</sup>, ZHAI Yu-chun(翟玉春)<sup>2</sup>, WANG Xin-hai(王新海)<sup>1</sup>, CHEN Lian(陈廉)<sup>3</sup>

(1. Institute of Nuclear Energy and Technology, Tsinghua University, Beijing 102201, China;  
 2. Department of Materials and Metallurgy, Northeastern University, Shenyang 110004, China;  
 3. Institute of Metal Research, The Chinese Academy of Sciences, Shenyang 110016, China)

**[Abstract]** Six kinds of Zr-based hydride alloy were designed. XRD analyses show that the main phase of  $Zr_{1-x}Ti_x$  ( $NiCoMnV$ )<sub>2.1</sub> alloy is Laves C15 when  $x$  is between 0 and 0.5, but the more the content of Ti, the more the Laves C14 phases. The amount of Laves C14 can be up to the amount of Laves C15 after substituted V and Fe by V-Fe alloy in  $Zr_{0.6}Ti_{0.4}$  ( $NiCoMnVFeCr$ )<sub>1.7</sub> alloy. The electrochemical measurements show that the discharge capacity of  $Zr_{0.9}Ti_{0.1}$  ( $NiCoMnV$ )<sub>2.1</sub> electrode is about 340 mA·h/g at 60 mA/g, but with increasing the amount of Ti, the discharge capacity of alloy electrode abruptly decreases; at 300 mA/g current density, its  $K_r$  can be up to 91%. The discharge capacity of  $Zr_{0.6}Ti_{0.4}$  ( $NiCoMn(V-Fe)Cr$ )<sub>1.62</sub> alloy electrode is about 200 mA·h/g at first cycle, the maximum capacity is more than that of the electrode with pure V, and about 315 mA·h/g.

**[Key words]** Zr-based hydride alloy; XRD; Laves phase; discharge capacity

**[CLC number]** TQ 343

**[Document code]** A

## 1 INTRODUCTION

With the development of economics and city traffics, more and more oil-powered vehicles appear, resulting more serious pollution to the city environment. Developing electric vehicles has become an important theme in the world. Rechargeable battery with high energy density is the key to the advanced electric vehicle.

It is obvious that high-capacity hydrogen storage alloys are essential to the NiMH batteries with high energy density. Since the commercialized AB<sub>5</sub> alloys are limited by their relatively low hydrogen storage capacity and low cycle life and others<sup>[1~3]</sup>, Zr-based AB<sub>2</sub> Laves phase alloys as a new generation of NiMH electrode materials, are attracting more and more interests for their high capacity and long cycle life<sup>[4~6]</sup>, but their low initial discharge capacity and high cost obstacle their developing. The object of this paper is to prime alloy composing, decrease cost, and substitute Ti for a part of Zr, and (V-Fe) alloy for pure V.

## 2 EXPERIMENTAL

The hydrogen storage elements can be classified as follows<sup>[7]</sup>:

- 1) increasing hydrogen storage, such as Mg, Ti, V, Zr, Nb, La;
- 2) raising kinetics, for example V, Mn, Zr(adjusting metal-hydride bond intensity);
- 3) improving surface properties, hole rate and specific conductance, for instance, Cr, Mo and W. According to above principle, six AB<sub>2</sub> type hydrogen

storage alloys were designed.

Alloy samples of  $Zr_{1-x}Ti_x$  (Ni, Co, Mn, V)<sub>2+ $\alpha$</sub>  ( $x = 0, 0.1, 0.3, 0.5, -0.1 < \alpha < 0.2$ ), ( $Zr_{0.6}Ti_{0.4}$ ) (Ni, Mn, Co, V, Fe, Cr)<sub>1.7</sub> and ( $Zr_{0.6}Ti_{0.4}$ ) (Ni, Mn, Co, (V-Fe), Cr)<sub>1.7</sub> (V, Fe substituted by V-Fe alloy) were prepared by vacuum induction furnace in the protective argon. In air, the as-cast alloy pieces were mechanically ground to powder of 74  $\mu$ m. In order to discuss easily, the samples were named:  $T_0$  ( $x = 0$ ),  $T_1$  ( $x = 0.1$ ),  $T_2$  ( $x = 0.3$ ),  $T_3$  ( $x = 0.5$ ),  $T_4$  (( $Zr_{0.6}Ti_{0.4}$ ) (Ni, Mn, Co, V, Fe, Cr)<sub>1.7</sub>),  $T_5$  (( $Zr_{0.6}Ti_{0.4}$ ) (Ni, Mn, Co, (V-Fe), Cr)<sub>1.7</sub>).

The electrochemical properties were determined at BT-2043 battery testing system made by Arbin Company, USA. Preparing total mass of 3.000 g powders of hydrogen storage alloy and nickel with the ratio of 1:3, the powders were cold-pressed into an electrode pellet of 25 mm in diameter. The pellet was sandwiched between two NiOOH/Ni(OH)<sub>2</sub> electrodes with excessive capacity, and then put into a beaker with 6 mol/L KOH containing 0.02 mol/L LiOH solution at (298  $\pm$  1) K, the sample was charged at current density of 60 mA/g for 8 h, and then discharged at the same current density to a cut-off voltage of 1 V.

After all electrodes were activated completely, the charge-discharge cycle life was measured at 300 mA/g current density. The cut-off voltage was 1 V.

XRD was carried out on the Rigaku D/max<sup>+</sup> Y<sub>A</sub> diffractometer. CuK $\alpha$  radiation and optical filtering

<sup>①</sup> [Foundation item] Project (715-004-0233) supported by the National Advanced Materials Committee of China

[Received date] 2001-10-18; [Accepted date] 2002-01-28;

with the graphite monochromator. SEM was finished on the S-360 type scanning electron microscope made in the Cambridge Instrument Ltd, and EDX carried out at the same time.

### 3 RESULTS AND DISCUSSION

#### 3.1 XRD analyses

Fig. 1 is the XRD patterns of  $T_4$  and  $T_5$ . From the plot, it is clear that  $T_4$  and  $T_5$  alloys consist of large amount of Laves C14, which is almost equal to Laves C15 and the content of Laves C15 in  $T_5$  is more than that of  $T_4$ .

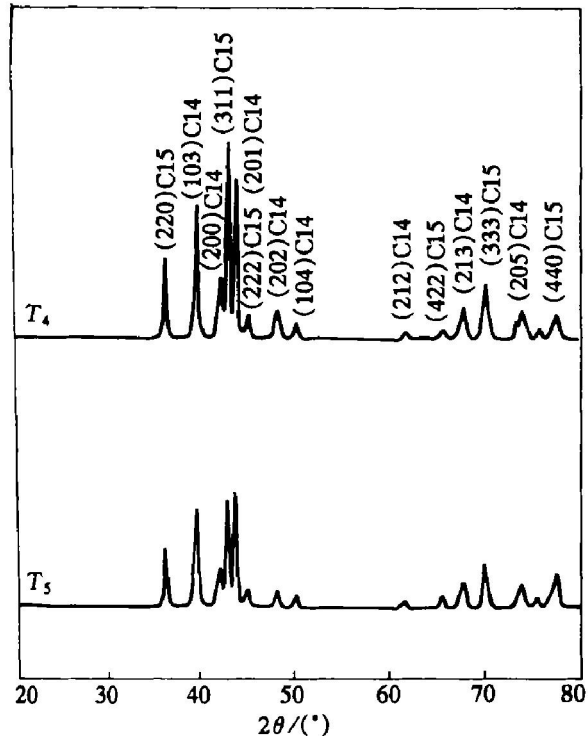


**Fig. 1** XRD patterns of Zr-based hydride alloy with different contents of V  
 $T_4$ — $Zr_{0.6}Ti_{0.4}(NiCoMnFeVCr)_{1.7}$ ;  
 $T_5$ — $Zr_{0.6}Ti_{0.4}(NiCoMn(Fe-V)Cr)_{1.62}$

Fig. 2 shows that all alloys consist of a great deal of cubic C15 Laves phase. In  $T_0$  alloy, the non-Laves phase is  $Zr_9Ni_{11}$ , while in  $T_1$  alloy, it is  $Zr_7Ni_{10}$ ; except  $T_1$  alloy, with increasing the content of  $T_i$ , the intensity of (311) peak is decreasing, however, the intensity of hexagonal C14 Laves phase rises.

#### 3.2 Laves phase formation

The ratio of atom radius is the main factor, which has effect on the formation of Laves phase. The theoretic radius ratio ( $R_A/R_B$ ) is 1.225, in fact, Laves C15 and Laves C14 are mixed in most situation. When the ratio  $R_A/R_B$  is more than 1.24, the alloy structure tends to Laves C15 type, while lower than 1.24, the crystal structure inclines to Laves C14<sup>[8]</sup>.

On the other hand, the crystal structure type is related to the alloy average outer electrons number

$n^{[9]}$ . In Zr-based and Ti-based alloys, when  $n < 4.67$ , no Laves phase formed; when  $4.67 < n < 5.4$ , the C15 Laves phase formed in Zr-based alloys, when  $n$  is between  $5.4 \sim 7.0$ , Laves C14 phase formed, while  $n$  is more than 7.0, Laves C15 phase formed in Zr-based and Ti-based alloy.

The crystal structure type is also related to the alloy average outer elements concentration ( $e/a$ )<sup>[10]</sup>. When  $e/a$  is more than 2.3, Laves C15 phase type is formed easily.

Table 1 is Laves phase formation conditions of six alloys. It shows that  $T_0$  and  $T_1$  alloys belong to Laves C15 type on the above principles, while the radius ratio of  $T_2$  and  $T_3$  are less than 1.24, which shows  $T_2$  and  $T_3$  alloy type are mixture of Laves C14 and C15, the result is the same as Fig. 2. It is clear that in  $T_4$  and  $T_5$  alloy, the crystal structures tend to Laves C14 phase, which is identical with Fig. 1.

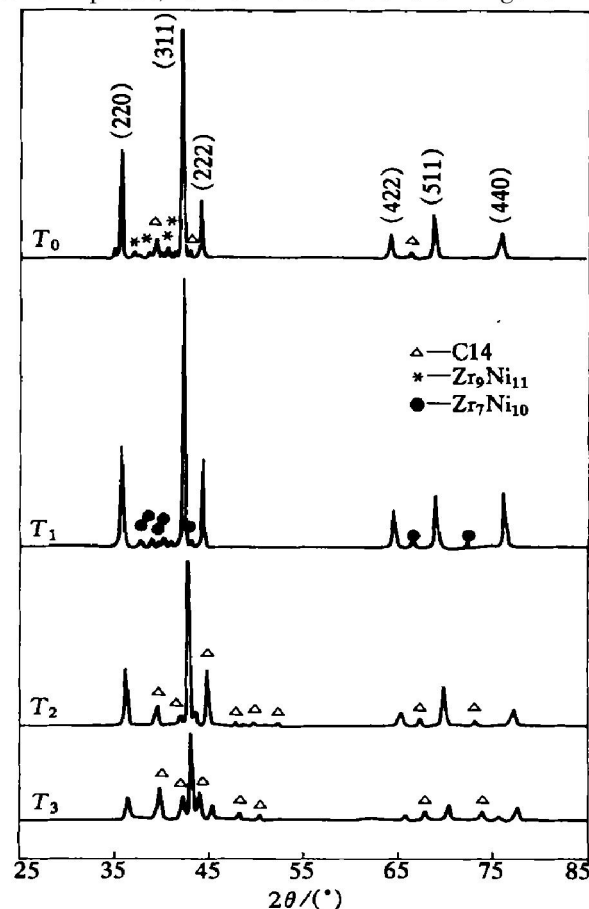


**Fig. 2** XRD patterns of  $Zr_{1-x}Ti_x(NiCoMnV)_{2.1}$  hydride alloys with different contents of Ti

**Table 1** Conditions of Laves phase formation

alloy	$R_A/R_B$	$e/a$	$n$
A	1.251	2.957	7.12
B	1.240	2.957	7.09
C	1.218	2.957	7.09
D	1.196	2.957	7.09
E	1.072	2.789	6.14
F	0.929	2.621	6.57

### 3.3 Electrode active behavior and discharge capacity

Fig. 3 shows the variation in discharge capacity with cycle number for different electrodes. It is clearly seen that the discharge capacities of  $T_0$  and  $T_1$  are obviously higher than others, in which  $T_1$  is little higher than  $T_0$ , up to 340 mA·h/g. But the maximum capacity of  $T_2$  is only 160 mA·h/g,  $T_3$  only 80 mA·h/g. The main reason is the content of Zr substituted by Ti, the more the Zr atom was replaced by Ti atom, the lower the stability of metal hydride<sup>[11]</sup>, which induces that hydrogen storage alloy desorbing hydrogen easily, was. Therefore, the discharge capacity decreases.

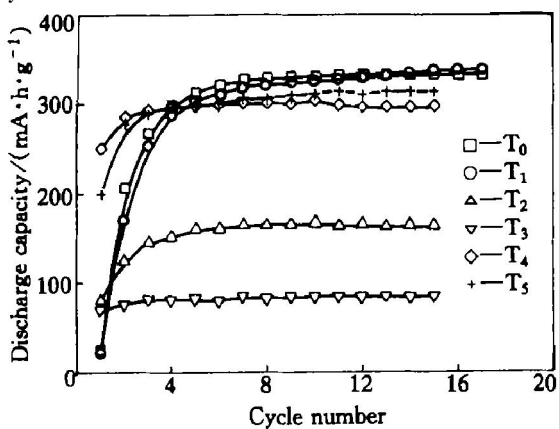


Fig. 3 Discharge capacity of hydride electrodes as function of cycle number

In Fig. 3, it can also be seen that the initial discharge capacity of  $T_5$  electrode is up to 200 mA·h/g, while that of  $T_4$  electrode is about 250 mA·h/g, which are higher than those of  $T_0$ ,  $T_1$ ,  $T_2$  and  $T_3$  electrodes. The more the laves C14 phase, the higher the initial discharging capacity.

### 3.4 Cycle life of electrodes

In Fig. 4, it can be seen that at 300 mA·h/g

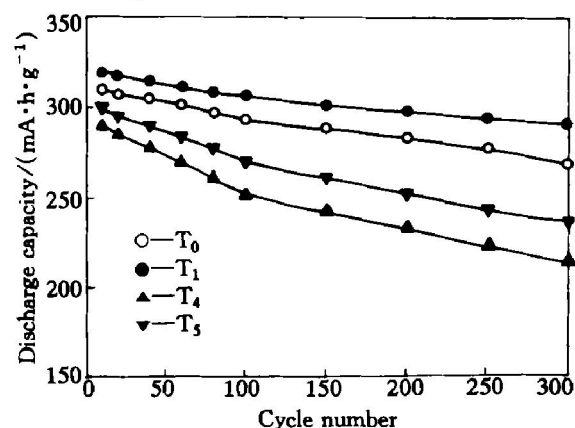


Fig. 4 Charge-discharge cyclife of different alloy electrodes

charge-discharge current density, the cycle stability of  $T_1$  is the best, the capacity keeping rate ( $K_r$ ) can be up to 91% after 300 cycles according to the following formula<sup>[12]</sup>, while  $T_4$  is the worst, whose  $K_r$  is only about 75%.

$$K_r = (C_{i,n} / C_{i,\max}) \times 100\%$$

where  $C_{i,n}$  is the discharge capacity at 'i' current density at 'n' cycle number, and  $C_{i,\max}$  is the maximum discharge capacity at 'i' current density.

## [ REFERENCES ]

- [1] Williems J G, Bunshow K H. From permanent magnets to rechargeable hydride electrodes [J]. *J Less Common Met.*, 1987, 129: 13– 20.
- [2] Suzuki K, Ranagihara N, Kawano H. Effect of rare earth composition on the electrochemical properties of  $Mm(NiMnAlCo)_5$  alloys [J]. *J Alloys Compd.*, 1993, 192: 173– 176.
- [3] Fukumoto Y, Miramuto M. Effect of the stoichiometric ratio on electrochemical properties of hydrogen storage alloys for nickel metal hydride batteries [J]. *Electrochimica Acta*, 1995, 40: 845.
- [4] Jung J H, Lee H H, Kim D M, et al. New activation process for  $Zr-Ti-Cr-Mn-V-Ni$  alloy electrodes—the hot-charging treatment [J]. *J Alloys Compd.*, 1997, 253– 254: 652– 655.
- [5] Liu B H, Jung J H, Lee H H. Improved electrochemical performance of  $AB_2$ -type metal hydride electrodes activated by the hot-charging process [J]. *J Alloys Compd.*, 1996, 245: 132– 141.
- [6] Iwakura C, Kim I, Matsue N, et al. Surface modification of Laves-phase  $ZrV_{0.5}Mn_{0.5}Ni$  alloy electrodes with alkaline solution containing potassium borohydride [J]. *Electrochemical Acta*, 1995, 40: 561– 563.
- [7] Pebler A, Gulbransen E A. Equilibrium studies on the systems  $ZrCr_2H_2$ ,  $ZrV_2H_2$ , and  $ZrMn_2H_2$  between 0° and 900° [J]. *Trans TMS-AIME*, 1967, 239: 1593.
- [8] Shinjiro W. Application of hydrogen absorbing alloys to secondary battery [J]. *Electric Furnace Steel*, 1995, 66 (2): 117– 120.
- [9] Toshiki K, Keizo O. Degradation and its mechanism of hydrogen absorbing alloys [J]. *Materia Japan*, 1997, 36 (4): 298– 301.
- [10] Thoma D J, Peredecko J H. A geometric analysis of solubility ranges in Laves phases [J]. *J Alloys Compd.*, 1995, 224: 330– 341.
- [11] Koichi M, Takayoshi S. Hydrogenation behavior of  $(Ti, Zr)(Ni, Mn, X)_2$  alloys [J]. *Electric Furnace Steel*, 1995, 66 (2): 97– 100.
- [12] WEN Ming-fen, ZHAI Yu-chun, CHEN Lian, et al. Effect of electroless plating nickel treatment on electrode properties of Zr-based  $AB_2$  type alloy [J]. *Trans Nonferrous Met Soc China*, 2001, 11(6): 856– 859.

(Edited by HUANG Jin-song)